Author Manuscript

Author Manuscript

Author Manuscript

Author Manuscript

HHS Public Access

Author manuscript

Biophys J. Author manuscript; available in PMC 2026 May 22.

Published in final edited form as:

Biophys J. 2026 November 17; 125(22): 6333–6345. doi:10.1016/j.bpj.2026.05.025.

Open Questions on Viral Frameshifting: Exploiting Structural Plasticity of the Frameshifting Element for Therapeutic Intervention

Stephanie Portillo-Ledesma[1],[4], **Samuel Lee**[5], **Alain Laederach**[6], **Tamar Schlick**[1],[2],[3],[4],[*]

[1]Department of Chemistry, New York University, 100 Washington Square East, Silver Building, New York, NY 10003, USA

[2]Courant Institute School of Mathematics, Computing, and Data Science, New York University, 251 Mercer St., New York, NY 10012, USA

[3]New York University-East China Normal University Center for Computational Chemistry, New York University Shanghai, Shanghai 200122, China

[4]Simons Center for Computational Physical Chemistry, New York University, 24 Waverly Place, Silver Building, New York, NY 10003, USA

[5]University of Pennsylvania, Philadelphia, PA 19104, USA

[6]Department of Biology, University of North Carolina at Chapel Hill, Chapel Hill, NC 27599, USA

Abstract

Programmed Ribosomal Frameshifting (PRF) is a specialized controlled-slippage genetic mechanism that viruses like SARS-CoV-2 and HIV-1 use to shift the reading frame during translation. This process is used in compact viral genomes to enhance their protein repertoire, maintain a precise balance of viral proteins necessary for successful replication, and enhance survival within a host. Because this mechanism is vital to the viral life cycle and remains consistent across strains, frameshifting has emerged as a promising therapeutic target for new antiviral therapeutic strategies. However, the complexity of the frameshifting process has posed many challenges that need to be addressed so that the relationship between cellular mechanisms and viral replication can be exploited for novel therapeutics. In this mini review, we introduce frameshifting mechanisms, define open questions being explored by many modeling and experimental studies, and illustrate how coarse-grained graphs have been used in our lab to study frameshifting mechanisms. Specifically, we describe how conformational landscapes, mutation designs of frameshifting elements, all-atom molecular dynamics and enhanced sampling

[*] Author to whom correspondence should be addressed: schlick@nyu.edu.

Author Contributions

T. S. wrote the original manuscript, made some of the figures, and contributed to some of the original work described. S. L. added some references and contributed to some of the original work described. S. P.-L. edited the manuscript and made some of the figures. A. L. contributed the section “Experimental Characterization of the Evolving Structural Ensembles”.

Declaration of Interests

The authors declare not competing interests.

Author Manuscript Author Manuscript Author Manuscript Author Manuscript

simulations have been combined with chemical mapping and functional experiments to advance studies on three viral systems employing −1 PRF: SARS-CoV-2, HIV-1, and Chikungunya.

Keywords

viral frameshifting; frameshifting elements; RNA folds; RNA motifs; frameshifting mutants; frameshifting efficiency

Introduction

Programmed Ribosomal Frameshifting (PRF) is a specialized controlled-slippage genetic mechanism that viruses like SARS-CoV-2 and HIV-1 use to shift the reading frame during translation. This process is used in compact viral genomes to enhance their protein repertoire, maintain a precise balance of viral proteins necessary for successful replication, and enhance survival within a host [1–6].

Specifically, for coronaviruses like SARS-CoV-2, retroviruses like HIV-1, and alpha viruses like Chikungunya (CHIKV), −1 PRF is employed to shift the translating frame backward by one nucleotide (in the 5′ direction) at a conserved slippery sequence [2, 3]. Besides common −1 PRF and +1 PRF mechanisms, less common −2 PRF and +2 PRF have also been observed [7]. In addition to viruses, PRF mechanisms are also present in some mammalian genes (e.g., antizyme/OAZ1, PEG10, Edr, Ma3) [8–11].

PRF functions as a critical mechanism for viral replication in several ways. By shifting the reading frame, the virus can produce out-of-frame proteins that are necessary for its lifecycle from a single mRNA sequence. PRF also allows the virus to maintain a precise balance between specific viral proteins (e.g., pp1a and pp1ab polyproteins in SARS-CoV-2) to ensure that the viral replication machinery functions correctly. PRF further serves as a critical switch in the viral replication program at specific, highly conserved, RNA locations; any disruption to the frameshifting process can halt viral production.

The RNA folds controlling these register shifts at the respective pausing sites are called frameshifting elements (FSEs). For different viruses, various FSE folds such as specific stem loops and pseudoknots (intertwined base pairs) are believed to be crucial for the requisite *pausing* associated with frameshifting [4, 6, 12–15]. See Table 1 for specific FSE structures identified experimentally for HIV-1, SARS and SARS-CoV-2, and other viruses. To illustrate, the FSE for SARS-CoV-2 is a small region in the open reading frame ORF1a,b region (Fig. 1, top) of the viral genome that codes for the polyproteins that initiate the cascade of viral protein synthesis. The 84-residue SARS-CoV-2 FSE (13462–13545 of the 29891 nt RNA genome) contains a 7-residue *slippery site* (UUUAAAC) and a 77-residue RNA (Fig. 1). When encountering ORF1b, out of register with respect to ORF1a, the ribosome backs up one nucleotide in the 5′ direction to define a different sequence of codons (Fig. 1). Because studies indicate correlations between the FSE conformational plasticity and frameshifting efficiency, it is likely that more complex conformational mechanisms are involved rather than a simple “barrier” [16–19]. Indeed, the discovery

Author Manuscript Author Manuscript Author Manuscript Author Manuscript

of many alternative conformations of the SARS-CoV-2 FSE [20–29] suggests a complex conformational and thermodynamic landscape.

Frameshifting as a Therapeutic Anti-Viral Target

Frameshifting mechanisms are vital to the viral life cycle and remain consistent across strains, where the FSE exhibits conserved sequence and structural regions [47–50]. For this reason, frameshifting has emerged as a promising therapeutic target for new antiviral therapeutic strategies [19, 51–53]. Indeed, many studies aim to exploit the vulnerabilities of ribosomal frameshifting to develop broad-spectrum treatments by small-molecule drugs and mutations to inhibit viral spread [54–59].

Already, small-molecule agents such as *1,4-diazepane derivative 10* (MTDB) (originally designed for SARS-CoV [18, 60, 61]), fluoroquinolone antibacterial *merafloxacin* [26], a phenyl thiourea C5 [62], and an amiloride [63] were found to hamper SARS-CoV-2 frameshifting. More recently, additional compounds have been reported to modulate coronavirus −1 PRF. These include the aminoglycoside geneticin [64], aminoquinazoline ligands from high-throughput small-molecule microarray screening [65], and a furo[2,3-b]quinoline derivative with activity against zoonotic coronaviruses [66]. In particular, the macrolide antibiotic carrimycin was shown to bind the FSE pseudoknot and decrease −1 PRF [67]. More recently, chemical probes targeting multiple binding sites in the SARS-CoV-2 frameshift pseudoknot have been pursued by structure-guided optimization [68].

Small molecules targeting non-coronaviral frameshift signals have also been studied. For example, HIV-1 frameshift RNA–targeted triazoles inhibit propagation of replication-competent and multidrug-resistant HIV in human cells [69].

Unlike viral proteins, which mutate rapidly and require continuous modifications, targeting the highly conserved viral genome residues has greater potential for robust and long-term therapeutic solutions [70–72]. Importantly, such RNA-targeting therapeutics and vaccines can disarm the origin of the infection rather than its products and be more effective in the long term. However, the complexity of the RNA molecule and the lagging science about its modeling, imaging, and drug screening compared to proteins pose challenges. Investigations of the RNA viral agent itself are crucial for understanding how the RNA invader replicates itself, is translated by the human ribosomal machinery, assembles, and synthesizes a suite of viral proteins that enable the continuation of its invasive trajectory. With technological improvements in RNA delivery systems, the rise of CRISPR-based gene editing systems [73, 74], and improved RNA modeling techniques [75–78], this *RNA focus is not only warranted but clearly successful*, as evident by recent mRNA-based vaccines.

Multiple Folds of the Frameshifting Element

Despite many ongoing studies, a mechanistic understanding of the frameshifting process and the impact of drugs on the frameshifting efficiency remain unclear. Complexity is intrinsic to the viral FSE and likely essential for its survival.

Author Manuscript Author Manuscript Author Manuscript Author Manuscript

An upstream attenuator hairpin (Fig. 1) may play a role in frameshifting [61, 62, 79, 80]. Because of the crucial relationship between the FSE conformational plasticity and the frameshifting mechanism [81], it is important to unravel the FSE conformational landscape. Besides the folds and mechanisms of the RNA FSE itself, important interactions occur between the FSE and the ribosome during viral protein synthesis. Advances on these many aspects of the frameshifting are needed so that frameshifting can be targeted for successful anti-viral therapeutic strategies.

Structural modeling, single molecule-techniques, high-throughput screening, SHAPE and DMS chemical mapping, in vitro functional assays, mutational analysis, and small drug binding studies are addressing these important questions concerning frameshifting mechanisms and the relationship between RNA FSE structure and frameshifting efficiency [82]. Frameshifting efficiency is defined as the percentage of the frameshifted population of protein products (from the −1 frame for −1 PRF) from the entire population (0 frame control products). The process is complex because multiple ribosomes encounter different lengths of RNA, which continuously fold and unfold during ribosomal translation depending on the accessible nucleotides not occluded by the ribosomes.

In Figure 2, we illustrate this concept of the evolving RNA transcript as encountered by translating ribosomes. The translating ribosome can stall at the FSE site when encountering a particular fold. Thus bulky pseudoknots encountered by the ribosome may promote frameshifting, and any alteration in the fold may alter the process.

This kinetic setting, well recognized for oligonucleotides [83], explains why conformational plasticity of the FSE has emerged as an important factor influencing frameshifting. Plasticity includes structural transitions among the different FSE folds, a result of the crowded RNA/ribosome environment. As ribosomal translation occurs, the number of residues upstream (5′) of the frameshifting site is reduced, and the RNA unfolds. Refolding of the transcript may occur as the ribosome moves away from the frameshifting site. The tension generated in the spacer region just 5′ of the frameshifting site has been identified as one factor triggering FSE structural transitions [84, 85].

Kinetic Versus Thermodynamic Stability of the Frameshifting Element

Complex kinetic, thermodynamic, and functional aspects of PRF have been intensively probed [17, 79, 80, 84, 86–89]. A force microscopy study of the very high frameshifting efficiency (80%) West Nile Virus (WNV) revealed complex and multiple dynamic pathways influenced by the tension generated by ribosomes [84]. Optical tweezers experiments complemented by molecular dynamics analysis showed that successive translating ribosomes mediate the folding and refolding of pseudoknots like those of FSEs and that structure coordination is important to rescue trapped folding intermediates [86].

These works and others [17, 87–89] clearly emphasize the complex interplay between kinetic and thermodynamic concepts for designing mutant FSEs by altering or suppressing the involvement of certain nucleotides to generate the desired FSE folding outcome [30, 90, 91]. For example, cryo-EM reconstructions of a ribosome stalled on the SARS-CoV-2

Author Manuscript Author Manuscript Author Manuscript Author Manuscript

pseudoknot show how the pseudoknot lodges at the mRNA entrance channel and exerts tension to promote frameshifting. Further, mutations that reduce pseudoknot stability can reduce this effect, consistent with altered frameshifting efficiency [44]. Other studies in SARS-CoV-2 and HIV contexts have used compensatory mutagenesis or stabilizing/destabilizing mutants to show that even modest de-stabilization in loops or base pairs in pseudoknot stems can alter frameshifting frequency [82, 87].

Importantly, folding intermediates involved in FSE translation also depend on the upstream and downstream nucleotides. For SARS-CoV-2, both upstream and downstream nucleotides may compete to define the stimulatory element (5′ and 3′ of the FSE) [79]. Building on the experimental work [79], we used equilibrium and kinetic modeling frameworks to show that the viral RNA adopts a dynamic ensemble of stem loop and pseudoknot structures that shift depending on flanking sequences and cellular context [31, 32, 85, 92]. In fact, a cascade-like conformational transitions is involved as ribosomal translation proceeds, with stem loops providing kinetic traps to the more thermodynamically stable pseudoknot [92]. Yan and Schlick [85] captured one of these transitions — between two 3-stem H-type pseudoknots — atomistically, revealing how the spacer region tension triggers a conformational transition and that the 3_6 pseudoknot is favored because it fits into the narrow ribosomal channel without clashes (Fig. 3). Accounting for kinetic stem formation in our mutation pipeline for the Chikungunya virus was found crucial in design of mutant FSEs. Thus, both local structural stability of the FSE RNA folds downstream and upstream of the shift site, and global environment of the RNA transcript associated with multiple ribosomes critically modulate −1 PRF efficiency.

Experimental Characterization of the Evolving Structural Ensembles

Single-molecule correlated chemical probing (smCCP) has emerged as a transformative approach for characterizing the structural ensembles of dynamic RNA elements, particularly viral PRFs [94, 95]. Unlike traditional bulk probing, which averages reactivity across a population, smCCP leverages “mutational profiling” (MaP) to record chemical modifications as mutations in cDNA during reverse transcription [96]. Because each sequencing read originates from a single RNA molecule, it is possible to identify concurrent mutations that reveal physical connectivity and structural heterogeneity [97]. This capability is critical for studying viral frameshifting elements such as in HIV-1 and SARS-CoV-2 where the equilibrium between alternative conformations, like a stable pseudoknot versus a hairpin, strictly regulates the ratio of viral proteins produced [98].

The most commonly used reagent is dimethyl sulfate (DMS), which methylates the Watson-Crick faces of unpaired adenines and cytosines [97, 99, 100]. In protocols such as DMS-MaPseq and DANCe-MaP (Deconvolution and Annotation of ribonucleic Conformational Ensembles) these methylations induce reverse transcriptase errors that encode mutations in the cDNA at the modified sites [97, 101, 102]. By analyzing the “correlated mutations, i.e. where two or more nucleotides are modified on the same individual RNA strand, it is possible to infer which bases are simultaneously exposed (single-stranded) in a specific conformation. The existence of a set of bases modified together in one sub-population

Author Manuscript Author Manuscript Author Manuscript Author Manuscript

of reads but protected in another indicates the presence of distinct, mutually exclusive structural states rather than a single static fold [102].

Advanced computational algorithms have been developed to deconvolute these complex experimental signals into distinct structural models. DRACO (Deconvolution of RNA Alternative Conformations), utilizes spectral clustering of these correlated mutation patterns to identify and quantify co-existing RNA structures without requiring prior knowledge of the fold [103]. Similarly, DANCe-MaP models single-molecule distinctness to characterize thermodynamic ensembles [94]. DREEM (Detection of RNA Folding Ensembles using Expectation Maximization) uses expectation maximation to identify alternative conformations [104]. These tools move beyond simple accessibility maps; they reconstruct alternative secondary structures by detecting long-range dependencies that appear only in specific subsets of the sequencing data. By moving beyond thermodynamic prediction of the RNA suboptimal ensemble, such methods allow direct experimental interrogation of these alternative states.

Open Questions

Some key ongoing questions in probing frameshifting mechanisms in viruses are focused broadly on how PRF functions as a critical mechanism for viral replication. Specific questions include the following:

- What is the role of different FSE folds and structural plasticity in the frameshifting process?
- How do kinetic traps and thermodynamic factors compete to define the FSE fold?
- How does the virus control these kinetic versus thermodynamic factors to ensure virus survival?
- What is the relationship between FSE fold and frameshifting efficiency? In other words, can we dissect the structural and energetic factors that influence frameshifting efficiency?
- How can we exploit PRF mechanisms to inhibit viral replication? What mutations and small-drug binding can we engineer to control the process?

Case Study: RAG-Based Studies on SARS-CoV-2, HIV-1, and CHIKV Integrating Modeling and Experimentation

As an example of body of complementary modeling and experimental work addressing frameshifting, we describe our group’s work on three −1 PRF systems since 2020: SARS-CoV-2, HIV-1, and CHIKV. The combination of modeling and experiments can be particularly fruitful because modeling can generate new hypotheses that can tested experimentally. The computational design of frameshifting element (FSE) mutants, in particular, has taught us how such predictions can succeed in both structural and functional alteration of FSE aspects, but also which ingredients complicate the story.

Author Manuscript Author Manuscript Author Manuscript Author Manuscript

RAG Description of RNA Motifs.

Our work on SARS-CoV-2, started during the 2020 Covid-19 pandemic, aimed to understand the conformational landscape of the FSE using a combination of complementary graph-based modeling and chemical reactivity and other experiments. We had just developed various computational tools using dual graphs, required to handle pseudoknots, within our coarse-grained framework of RNA secondary structures called RNA-As-Graphs or RAG [105–109].

The coarse-grained representations simplify RNA motifs, allowing us to classify many 2D structures that have the same topological features into one class (see Fig. 1). The graph notation V_n refers to the graph vertex number V and a graph label n where all graphs of V vertices are ordered by increasing compactness. The compactness of the graph is described by the second eigenvalue of the Laplacian matrix that describes graph connectivity [105]. Besides cataloging graph motifs and associating motifs with solved RNAs in our graph library using tree or dual graphs [110–112], the RAG framework led to applications to estimate the motif universe of RNAs and predict RNA-like motifs [112, 113]. Practical applications of graph partitioning methods include determining repeating submotifs in RNAs, using submotifs for design of new RNAs [111, 112, 114–119], and predicting 3D topologies of RNAs from primary and/or secondary structure information [120].

Already in the early days of the pandemic, several groups have explored FSE structure by modeling [20, 28–30, 121], Selective 2′-Hydroxyl Acylation by Primer Extension (SHAPE) [122, 123] and DMS structure probing experiments [21–27], NMR [124, 125], X-ray crystallography [43, 45, 126], SAXS and SAXS-guided modeling [127], Cryo-EM [22, 93], and other biophysical mutational profiling and scanning approaches [61, 128, 129].

The FSE of SARS-CoV-2 was predominantly characterized as a 3-stem hairpin (H-type) pseudoknot with colinear Stems 1 and 2 intertwined via a pseudoknot and perpendicular Stem 3. This association has persisted since the original SARS-CoV frameshift-signal characterization [130, 131], and the SARS-CoV element differs in only one base from the SARS-CoV-2 FSE (residue A13533 in Covid-19 is C in SARS, Fig. 1); see also [61]. However, depending on the modeling software and experimental technique, alternative secondary structures have been reported for SARS-CoV-2, both pseudoknotted and unknotted [20–29].

To explore the conformational landscapes of FSEs broadly, we developed and applied several computational tools. These include: *conformational landscapes* [31]; *computational design of FSE mutants by inverse folding* [30, 132], with a recent addition of an integrative mutation pipeline that accounts for kinetic traps [133]; and *atomistic molecular dynamics* [32], augmented by *enhanced sampling* [85] simulations of wildtype and mutant systems to determine their stability and explore dynamic transitions among RNA folds [85]. Classic phylogenetic analysis to determine virus conservation across species and to relate FSE sequence to fold evolution can also be helpful for interpreting FSE landscapes [47]. Together with SHAPE and DMS reactivity experiments, Luciferase functional assays for frameshifting efficiency (FE) measurements, and other experiments to probe the relationship

Author Manuscript Author Manuscript Author Manuscript Author Manuscript

between FSE fold and FE [80], these studies have addressed some of the open questions above for several −1 PRF viral systems.

Conformational Landscapes.

In conformational landscapes, we explore the RNA folds as the sequence increases by adding upstream (5′) residues to mimic structures available to the translating ribosome before it has passed the stimulatory region, and downstream (3′) residues to mimic RNA refolding; motifs using graphs are used to characterize the percentage of each fold at a given RNA length, weighted by its Boltzmann energy factor $p_i \propto \exp -E_i/(k_B T)$. Here the probability p_i of each conformation i is proportional to the Boltzmann factor where E_i is the free energy estimate of conformation i, and k_B and T are the Boltzmann constant and temperature, respectively [31, 92]. These landscapes can be predicted using various 2D folding programs, and guided by SHAPE or DMS reactivity data. Subject to the usual approximations of 2D folding algorithms for RNA, the resulting landscapes estimate the repertoire of the folds that may be available to the FSE and suggest how folds evolve with sequence length. They can also explore the effect of the downstream and upstream regions on the FSE motifs.

Figures 4 and 5 show the FSE and −1 PRF sequences for CHIKV [133] and HIV-1 [134] and computed conformational landscapes (expanding downstream for CHIKV and both upstream and downstream for HIV-1), along with observed RNA folds, depicted as RNA dual graphs, and their irreducible partitions (for HIV-1). CHIKV (Figure 4B and C) shows that at shorter lengths (43–54 nt), the 2_2 motifs dominate, with 2_2L becoming prevalent at around 47 nt. This 2_2L motif is contained within a simple 1_1 stem-loop structure. By 55 nt, the structure shifts to a slightly more complex 3_1 motif. At 61 nt, the addition of nucleotides enables formation of a pseudoknot-containing 4_12 motif (1_1 + 3_6), which becomes dominant for the rest of the landscape. This transition is driven by new long-range interactions and agrees with experiments showing that the 3_6 pseudoknot is essential for CHIKV frameshifting. Minimal mutations can bias the FSE conformation toward specific conformations (Figure 4D): pseudoknot 3_6 (red), nested stem loop 2_2L (green), nested stem loop 2_2R (orange), or two separated stems 2_1 (purple).

HIV shows that the 2_2 stem–loop motif is highly stable and dominates the FSE across sequence lengths (Figure 5B and C). While some pseudoknots (e.g., 4_17) still appear, the core FSE consistently preserves key elements, especially the upper stem and ACAA hairpin, across most dominant motifs. Minimal mutations can transform the conformation into a pseudoknot-containing 2_3 dual graph or a two-stem 2_1 dual graph. Thus, overall, the landscapes emphasize that distinct structural families can become accessible or unavailable as additional flanking nucleotides are added.

For SARS-CoV-2, this framework motivated our SHAPE-guided modeling in which the two recurrent pseudoknots and 3-way junction emerged as major folds as shown in Figure 1 (two 3-stem pseudoknotted RNAs, 3_6 and 3_3 in our dual graph notation, and the unknotted 3-way junction RNA (3_5)) [31]. Longer sequence contexts which include AH incorporate upstream elements [31, 92, 126]. For CHIKV, we associate length regimes with distinct fold families in our landscape [133]. For HIV-1, the folds are simpler but nonetheless also

Author Manuscript Author Manuscript Author Manuscript Author Manuscript

variable. The landscapes lead naturally to target mutant folds as a way to alter FSE fold stability and frameshifting efficiency.

In complementary evolutionary analysis [47] of 23 representative Alpha and Beta coronaviruses, we described landscapes for each virus's FSE by a variety of pseudoknots, stem loops, and junctions, with the pseudoknot motif robust. We correlated evolutionary changes to recurring mutations and linked them to the tuning of frameshifting efficiency. The recent experimental study [80] further attempted to relate four −1 PRF elements to their frameshifting efficiencies. We observed that −1 PRF efficiency does not always increase with the number of alternative conformations, and that canonical alternative stem formation tends to correlate with better frameshifting elements. In particular, sequence elements upstream of the attenuator hairpin could markedly modulate (enhance or suppress) viral frameshifting [125, 126].

FSE Mutant Design by RAG Inverse Folding and Integrative Kinetic/Thermodynamic Pipeline.

For SARS-CoV-2, these landscapes led us to design mutants by our RAG Inverse folding algorithm [132]: we apply a genetic algorithm to determine minimal mutations that convert one RNA topology onto another so that the fold remains stable for a range of lengths. The double mutants shown in Fig. 1 attempt to lock the FSE at one conformation (see [30] and accompanying New & Notable commentary [135]). Subsequent atomic MD simulations showed the mutant that stabilizes the 3_6 pseudoknot suppresses the I to L-shaped transitions [32]. Importantly, experimental characterization of our three mutants confirmed that these designed mutants stabilize one conformation over all others [31]. Most exciting, Luciferase assay measurements showed that these mutants nearly abolish frameshifting [82]. These results underscore the essential role that structural plasticity, rather than thermodynamic stability, has on frameshifting and suggest that suppressing structural transitions may be therapeutically advantageous to delay viral infection.

Recently, we added a kinetic analysis component to the mutation design to analyze the secondary-structure evolution in time [133]. This component was essential to iterate on one CHIKV mutant design to inhibit the kinetically trapped stem loops instead of the thermodynamically stable pseudoknot. The added step can help check mutation designs before they are subjected to experimental testing. Ongoing experiments are testing our minimal FSE mutants for HIV-1 and CHIKV.

Atomistic MD and Enhanced Sampling Simulations.

Exploring insights from the MD simulations on how the flexible Stem 2 may be involved in a switch between these conformations and associations with the ribosome during protein translation, Yan and Schlick [85] recently captured the transition between the two pseudoknots using atomistic transition path sampling combined with Markov state modeling (see Figure 3). The favored 3_3 pseudoknot at long lengths leads to clashes with the ribosome as the ribosome approaches the pause site; the spacer region tension then triggers a conformational transition between the two H-type pseudoknots, 3_3 to 3_6, and helps the latter position itself well within the narrow ribosomal channel. The studies also describe a

Author Manuscript Author Manuscript Author Manuscript Author Manuscript

heterogeneous multi-hub transition pathways, provide free energies for specific paths, and explain why the 3_6 pseudoknot is the experimentally favored fold: this pseudoknot fits optimally within the narrow ribosomal channel without clashes, whereas the 3_3 pseudoknot experiences many residue clashes.

Conclusions

The studies and ideas summarized here emphasize the importance of the FSE plasticity and the complexity of the FSE fold landscape (Figure 2). The relationship between FSE structure and frameshifting efficiency is not straightforward, and kinetic versus thermodynamic factors govern the folding of the FSE and the frameshifting process.

The combined works of experimental and modeling researchers broadly highlight three possible directions for novel therapeutic avenues to target frameshifting as an anti-viral target: (1) alter the FSE conformational state (fold) itself; (2) interfere with the FSE structural transformations; and/or (3) interrupt the FSE/ribosome interactions. All these avenues can be achieved with suitable FSE mutations and/or small-molecule drugs. Combinations of these avenues may be particularly powerful.

A better characterization of frameshifting elements also has biotechnological applications in packaging gene therapies or controlling stoichiometric protein expression ratios. However, cellular mechanisms must be advanced to administer these type of changes in human cells as intended.

Ongoing research is continuing to address these therapeutic avenues as well as the dynamic mechanisms associated with frameshifting. Given the inevitable rise of viral threats, pursuing these scientific and medical questions could lead to more immediate and diverse tools for the next pandemic.

Acknowledgments

This work is supported by the National Science Foundation Award DMS-215777 and CHE-2330628 from the Division of Mathematical Sciences and the Division of Chemistry, the National Institute of Health award R35-GM122562 from the National Institute for General Medical Sciences, and the Philip Morris International to T.S. T.S. also acknowledges support from the Simons Foundation, Award MPS-T-MPS-00839534 to MET, in conjunction with the Simons Center for Computational Physical Chemistry at NYU. We thank Dr. Rui Wang for creating the dual graphs for the RSV images in Table 1.

Abbreviations used:

FSE	frameshifting element
MSA	Multiple Sequence Alignment
PRF	programmed ribosomal frameshifting
RAG	RNA-As-Graphs
FE	frameshifting efficiency
CHIKV	Chikungunya

Author Manuscript Author Manuscript Author Manuscript Author Manuscript

NMR	Nuclear Magnetic Resonance
SAXS	Small Angle X-ray Scattering

References

[1]. Hill CH and Brierley I. Structural and functional insights into viral programmed ribosomal frameshifting. Annu. Rev. Virol, 10:217–242, 2023.

[2]. Brierley I. Ribosomal frameshifting on viral RNAs. J. Gen. Virol, 76:1885–1892, 1995.

[3]. Atkins J, Loughran G, Bhatt P, Firth A, and Baranov P. Ribosomal frameshifting and transcriptional slippage: From genetic steganography and cryptography to adventitious use. Nucleic Acids Res., 44(15):7007–7078, 2016.

[4]. Staple D and Butcher S. Solution structure of the HIV-1 frameshift inducing stem–loop RNA. Nucleic Acids Res., 31:4326–4331, 2003.

[5]. Dinman JD. Mechanisms and implications of programmed translational frameshifting. WIREs RNA, 3(5):661–673, 2012.

[6]. Ramamonjiharisoa MBM and Liu S. Biological significance and therapeutic promise of programmed ribosomal frameshifting. Int. J. Mol. Sci, 26(3):1294, 2025.

[7]. Riegger RJ and Caliskan N. Thinking outside the frame: impacting genomes capacity by programmed ribosomal frameshifting. Front. Mol. Biosci, 9:842261, 2022.

[8]. Matsufuji S, Matsufuji T, Miyazaki Y, Murakami Y, Atkins JF, Gesteland RF, and Hayashi S. Autoregulatory frameshifting in decoding mammalian ornithine decarboxylase antizyme. Cell, 80(1):51–60, 1995.

[9]. Clark MB, Janicke RPJ, Godfrey NAJ, Ghersi RHC, and Mattick JS. Mammalian gene PEG10 expresses two reading frames by high efficiency −1 frameshifting in embryonic-associated tissues. J Biol. Chem, 282(52):37359–37369, 2007.

[10]. Manktelow E, Shigemoto K, and Brierley I. Characterization of the frameshift signal of Edr, a mammalian example of programmed −1 ribosomal frameshifting. Nucleic Acids Res., 33(5):1553–1563, 2005.

[11]. Wills NM, Moore B, Hammer A, Gesteland RF, and Atkins JF. A functional −1 ribosomal frameshift signal in the human paraneoplastic Ma3 gene. J Biol. Chem, 281(11):7082–7088, 2006.

[12]. Brierley I, Digard P, and Inglis S. Characterization of an efficient coronavirus ribosomal frameshifting signal: requirement for an RNA pseudoknot. Cell, 57:537–547, 1989.

[13]. Somogyi P, Jenner A, Brierley I, and Inglis S. Ribosomal pausing during translation of an RNA pseudoknot. Mol. Cell. Biol, 13:6931–6940, 1993.

[14]. Lopinski J, Dinman J, and Bruenn J. Kinetics of ribosomal pausing during programmed −1 translational frameshifting. Mol. Cell. Biol, 20:1095–1103, 2000.

[15]. Kim H, Liu F, Fei J, Bustamante C, Gonzalez R, and Tinoco I. A frameshifting stimulatory stem loop destabilizes the hybrid state and impedes ribosomal translocation. Proc. Nat. Acad. Sci., USA, 111:5538–5543, 2014.

[16]. Namy O, Moran S, Stuart D, Gilbert R, and Brierley I. A mechanical explanation of RNA pseudoknot function in programmed ribosomal frameshifting. Nature, 441:244–247, 2006.

[17]. Ritchie D, Foster A, and Woodside M. Programmed −1 frameshifting efficiency correlates with rna pseudoknot conformational plasticity, not resistance to mechanical unfolding. Proc. Nat. Acad. Sci., USA, 109:16167–16172, 2012.

[18]. Ritchie D, Soong J, Sikkema K, and Woodside M. Anti-frameshifting ligand reduces the conformational plasticity of the SARS virus pseudoknot. J. Amer. Chem. Soc, 136:2196–2199, 2014.

[19]. Kelly J, Woodside M, and Dinman J. Programmed −1 ribosomal frameshifting in coronaviruses: A therapeutic target. Virology, 554:75–82, 2021.

[20]. Trinity L, Wark I, Lansing L, Jabbari H, and Stege U. Shapify: Paths to SARS-CoV-2 frameshifting pseudoknot. PLOS Comput. Biol, 19:e1010922, 2023.

Author Manuscript Author Manuscript Author Manuscript Author Manuscript

[21]. Huston N, Wan H, Strine M, Tavares R, Wilen C, and Pyle A. Comprehensive in vivo secondary structure of the SARS-CoV-2 genome reveals novel regulatory motifs and mechanisms. Mol. Cell, 81:584–598.e5, 2021.

[22]. Zhang K, Zheludev I, Hagey R, Wu M, Haslecker R, et al. Cryo-EM microscopy and antisense targeting of the 28-kDa frameshift stimulation element from the SARS-CoV-2 RNA genome. Nat. Struc. Mol. Biol, 2021.

[23]. Lan TCT, Allan MF, Malsick LE, Woo JZ, Zhu C, Zhang F, Khandwala S, Nyeo SSY, Sun Y, Guo JU, Bathe M, Näär A, Griffiths A, and Rouskin S. Secondary structural ensembles of the SARS-CoV-2 RNA genome in infected cells. Nature Comm., 13:1128, 2022.

[24]. Manfredonia I, Nithin C, Ponce-Salvatierra A, Ghosh P, Wirecki TK, Marinus T, Ogando NS, Snijder EJ, van Hemert MJ, Bujnicki JM, and Incarnato D. Genome-wide mapping of SARS-CoV-2 RNA structures identifies therapeutically-relevant elements. Nucl. Acids Res, 48(22):12436–12452, 2020.

[25]. Morandi E, Manfredonia I, Simon LM, Anselmi F, van Hemert MJ, Oliviero S, and Incarnato D. Genome-scale deconvolution of RNA structure ensembles. Nature Meth., 18:249–252, 2021.

[26]. Sun L, Li P, Ju X, Rao J, Huang W, Ren L, Zhang S, Xiong T, Xu K, Zhou X, Gong M, Miska E, Ding Q, Wang J, and Zhang QC. In vivo structural characterization of the SARS-CoV-2 RNA genome identifies host proteins vulnerable to repurposed drugs. Cell, 184:1865–1883.e20, 2021.

[27]. Iserman C, Roden CA, Boerneke MA, Sealfon RSG, McLaughlin GA, Jungreis I, Fritch EJ, Hou YJ, Ekena J, Weidmann CA, Theesfeld CL, Kellis M, Troyanskaya OG, Baric RS, Sheahan TP, Weeks KM, and Gladfelter AS. Genomic RNA elements drive phase separation of the SARS-CoV-2 nucleocapsid. Mol. Cell, 80(6):1078–1091, 2020.

[28]. Andrews R, O'Leary C, Tompkins V, Peterson J, Haniff H, Williams C, Disney M, and Moss W. A map of the SARS-CoV-2 RNA structurome. NAR Genom. Bioinform, 3(2):lqab043, 2021.

[29]. Ahmed F, Sharma M, Al-Ghamdi A, Al-Yami S, Al-Salami AM, Refai MY, Warsi MK, Howladar SM, and Baeshen MN. A comprehensive analysis of cis-acting RNA elements in the SARS-CoV-2 genome by a bioinformatics approach. Front. Genet, 11:1385, 2020.

[30]. Schlick T, Zhu Q, Jain S, and Yan S. Structure-altering mutations of the SARS-CoV-2 frameshifting RNA element. Biophys. J, 120:1040–1053, 2021.

[31]. Schlick T, Zhu Q, Dey A, Jain S, Yan S, and Laederach A. To knot of not to knot: Multiple conformations of the SARS-CoV-2 frameshifting RNA element. J. Amer. Chem. Soc, 143:11404–11422, 2021.

[32]. Yan S, Zhu Q, Jain S, and Schlick T. Length-dependent motions of SARS-CoV-2 frameshifting RNA pseudoknot and alternative conformations suggest avenues for frameshifting suppression. Nature Comm., 13:4284, 2022.

[33]. Rolband L, Beasock D, Wang Y, Shu Y-G, Dinman JD, Schlick T, Zhou Y, Kieft JS, Chen S-J, Bussi G, Oukhaled A, Gao X, Šulc P, Binzel D, Bhullar AS, Liang C, and Guo P. Biomotors, viral assembly, and RNA nanobiotechnology: Current achievements and future directions. Comp. Struc. Biotech. J, 20:6120–6137, 2022.

[34]. Staple DW and Butcher SE. Solution structure and thermodynamic investigation of the HIV-1 frameshift inducing element. J. Mol. Biol, 310(5):1109–1123, 2005.

[35]. Dulude D, Baril Y, and Brakier-Gingras L. Characterization of the frameshift stimulatory signal controlling a programmed −1 ribosomal frameshift in the human immunodeficiency virus type 1. Nucleic Acids Res., 30(23):5094–5102, 2002.

[36]. Marcheschi RJ, Staple DW, and Butcher SE. Programmed ribosomal frameshifting in SIV is induced by a highly structured RNA stem-loop. J. Mol. Biol, 373(3):652–663, 2007.

[37]. Nixon PL, Rangan A, Kim Y-G, Rich A, Hoffman DW, Hennig M, and Giedroc DP. Solution structure of a luteoviral p1–p2 frameshifting mRNA pseudoknot. J. Mol. Biol, 322(3):621–633, 2002.

[38]. Pallan PS, Marshall AP, Nixon PL, and Giedroc DP. Crystal structure of a luteoviral RNA pseudoknot and model for a minimal ribosomal frameshifting motif. Biochem., 44(34):11315–11322, 2005.

Author Manuscript Author Manuscript Author Manuscript Author Manuscript

[39]. Cornish PV, Stammler MA, and Giedroc DP. The global structures of a wild-type and poorly functional plant luteoviral mRNA pseudoknot are essentially identical. RNA, 12(11):1959–1969, 1969.

[40]. Egli M, Minasov G, Su L, and Rich A. Metal ions and flexibility in a viral RNA pseudoknot at atomic resolution. Proc. Natl. Acad. Sci. U.S.A, 99(7):4302–4307, 2002.

[41]. Shen LX and Tinoco I Jr. The structure of an RNA pseudoknot that causes efficient frameshifting in mouse mammary tumor virus. J. Mol. Biol, 247(5):963–978, 1995.

[42]. Michiels PJA, Versleyen A, Pleij CWA, and Hilbers CW. Solution structure of the pseudoknot of srv-1 RNA, involved in ribosomal frameshifting. J. Mol. Biol, 310(5):1109–1123, 2002.

[43]. Roman C, Lewicka A, Koirala D, Li N-S, and Piccirilli JA. The SARS-CoV-2 programmed −1 ribosomal frameshifting element crystal structure solved to 2.09 å using chaperone-assisted RNA crystallography. ACS Chem. Biol, 16(8):1469–1481, 2021.

[44]. Bhatt PR, Scaiola A, Loughran G, Leibundgut M, Kratzel A, Meurs R, Dreos R, O'Connor KM, McMillan A, Bode JW, Thiel V, Gatfield D, Atkins JF, and Ban N. Structural basis of ribosomal frameshifting during translation of the SARS-CoV-2 RNA genome. Science, 372(6548):1306–1313, 2021.

[45]. Jones CP and Ferré-D'Amaré AR. Crystal structure of the severe acute respiratory syndrome coronavirus 2 (SARS-CoV-2) frameshifting pseudoknot. RNA, 28(2):239–249, 2022.

[46]. Jones CP and Ferré-D'Amaré AR. Structural switching dynamically controls the doubly pseudoknotted rous sarcoma virus–programmed ribosomal frameshifting element. Proc. Nat. Acad. Sci. USA, 122(14):e2418418122, 2025.

[47]. Yan S, Zhu Q, Hohl J, Dong A, and Schlick T. Evolution of coronavirus frameshifting elements: Competing stem networks explain conservation and variability. Proc. Natl. Acad. Sci. USA, 120(20):e2221324120, 2023.

[48]. Yang SL, DeFalco L, Wang S, Wong YH, Han J, Mok CK, Tan KY, Lim SY, Zhao Z, Zhang Y, Lim JJA, Xiang JS, Sobota R, Wang L-F, Chu JJH, Merits A, Huber RG, and Wan Y. A conserved long-range RNA interaction in SARS-CoV-2 recruits ADAR1 to enhance virus proliferation, ty = JOUR, url = https://doi.org/10.1038/s41467-025-63297-2, volume = 16, year = 2025, bdsk-url-1 = 10.1038/s41467-025-63297-2. Nature Comm., (1):8460.

[49]. Dinman JD, Richter S, Plant EP, Taylor RC, Hammell AB, and Rana TM. The frameshift signal of hiv-1 involves a potential intramolecular triplex rna structure. Proc. Nat. Acad. Sci. USA, 99(8):5331–5336, 2002.

[50]. Huang X, Yang Y, Wang G, Cheng Q, and Du Z. Highly conserved rna pseudoknots at the gag-pol junction of hiv-1 suggest a novel mechanism of −1 ribosomal frameshifting. RNA, 20(5):587–593, 2014.

[51]. Dinman J, Ruiz-Echevarria M, Czaplinski K, and Peltz S. Peptidyl-transferase inhibitors have antiviral properties by altering programmed −1 ribosomal frameshifting efficiencies: Development of model systems. Proc. Nat. Acad. Sci., USA, 94:6606–6611, 1997.

[52]. Kinzy T, Harger J, Carr-Schmid A, Kwon J, Shastry M, Justice M, and Dinman J. New targets for antivirals: The ribosomal A-site and the factors that interact with it. Virology, 300:60–70, 2002.

[53]. Anokhina VS and Miller BL. Targeting ribosomal frameshifting as an antiviral strategy: from HIV-1 to SARS-CoV-2. Acc. Chem. Res, 54:3349–3361, 2021.

[54]. Garcia-Miranda P, Becker JT, Benner BE, Blume A, Sherer NM, and Butcher SE. Stability of hiv frameshift site rna correlates with frameshift efficiency and decreased virus infectivity. J. Virol, 90(15):6906–6917, 2016.

[55]. Neupane K, Munshi S, Zhao M, Ritchie DB, Ileperuma SM, and Woodside MT. Anti-frameshifting ligand active against SARS coronavirus-2 is resistant to natural mutations of the frameshift-stimulatory pseudoknot. J. Mol. Biol, 432:5843–5847, 2020.

[56]. Munshi S, Neupane K, Ileperuma SM, Halma MTJ, Kelly JA, Halpern CF, Dinman JD, Loerch S, and Woodside MT. Identifying inhibitors of −1 programmed ribosomal frameshifting in a broad spectrum of coronaviruses. Viruses, 14:177, 2022.

[57]. Zimmer MM, Kibe A, Rand U, Pekarek L, Ye L, Buck S, Smyth RP, Cicin-Sain L, and Caliskan N. The short isoform of the host antiviral protein ZAP acts as an inhibitor of SARS-CoV-2 programmed ribosomal frameshifting. Nat. Commun, 12:7193, 2021.

Author Manuscript Author Manuscript Author Manuscript Author Manuscript

[58]. Toews S, Ceylan B, Wacker A, Ken M, and Schwalbe H. Integrative in silico and in vitro screening of low molecular weight compounds targeting sars-cov-2 rna elements. ChemBioChem, 26(24):e202500668, 2025.

[59]. Kovachka S, Wang J, Taghavi A, Jia Y, Asaba T, Wolff KC, Martin M, Yang X, Meyer SM, Ottilie S, Heacock M, Cheng Z, McNamara CW, Dubey G, Chatterjee AK, Chanda S, Gallego J, Childs-Disney JL, and Disney MD. J. Am. Chem. Soc, (41):37460–37479, publisher = American Chemical Society, title = Covalent Probes Reveal Small–Molecule Binding Pockets in Structured RNA and Enable Bioactive Compound Design, volume = 147, year = 2025, Bdsk–Url–1 = 10.1021/jacs.5c11898.

[60]. Park S, Kim Y, and Park H. Identification of RNA pseudoknot-binding ligand that inhibits the −1 ribosomal frameshifting of SARS-coronavirus by structure-based virtual screening. J. Amer. Chem. Soc, 133:10094–10100, 2011.

[61]. Kelly J, Olson A, Neupane K, Munshi S, Emeterio J, Pollack L, Woodside M, and Dinman J. Structural and functional conservation of the programmed −1 ribosomal frameshift signal of SARS coronavirus 2 (SARS-CoV-2). J. Biol. Chem, 295:10741–10748, 2020.

[62]. Haniff H, Tong Y, Liu X, Chen J, Suresh B, Andrews R, Peterson J, et al. Targeting the SARS-CoV-2 RNA genome with small molecule binders and ribonuclease targeting chimera (RIBOTAC) degraders. ACS Cent. Sci, 6:1713–1721, 2020.

[63]. Swanson Hay EG, Maille MM, Zafferani M, Puray-Chavez M, Xia M, Luu TB, Muralidharan D, Li M-L, Brewer G, Kutluay SB, Mouzakis KD, and Hargrove AE. Sars-cov-2 antivirals identified from small molecule modulators of programmed 1 ribosomal frameshifting. ACS Infect. Dis, 2026.

[64]. Varricchio C, Mathez G, Pillonel T, Bertelli C, Kaiser L, Tapparel C, Brancale A, and Cagno V. Geneticin shows selective antiviral activity against SARS-CoV-2 by interfering with programmed −1 ribosomal frameshifting. Antiviral Res., 208:105452, 2022.

[65]. Yang M, Olatunji FP, Rhodes C, Balaratnam S, Dunne-Dombrink K, Seshadri S, Liang X, Jones CP, Le Grice SFJ, Ferré-D'Amaré AR, and Schneekloth JS Jr. Discovery of small molecules targeting the frameshifting element RNA in SARS-CoV-2 viral genome. ACS Med. Chem. Lett, 14(6):757–765, 2023.

[66]. Ahn D-G, Yoon GY, Lee S, Ku KB, Kim C, Kim K-D, Kwon Y-C, Kim G-W, Kim B-T, and Kim S-J. A novel frameshifting inhibitor having antiviral activity against zoonotic coronaviruses. Viruses, 13(8):1639, 2021.

[67]. Li H, Li J, Li J, et al. Carrimycin inhibits coronavirus replication by decreasing the efficiency of programmed −1 ribosomal frameshifting through directly binding to the RNA pseudoknot of viral frameshift-stimulatory element. Acta Pharm. Sin. B, 14(6):2567–2580, 2024.

[68]. Ceylan B, Adam J, Toews S, Kaiser F, Dörr J, Scheppa D, Tants J-N, Smart A, Schoth J, Philipp S, Stirnal E, Ferner J, Richter C, Sreeramulu S, Caliskan N, Schlundt A, Weigand JE, Göbel M, Wacker A, and Schwalbe H. Optimization of structure-guided development of chemical probes for the pseudoknot RNA of the frameshift element in SARS-CoV-2. Angew. Chem. Int. Ed, 64:e202417961, 2025.

[69]. Hilimire TA, Chamberlain JM, Anokhina V, Bennett RP, Swart O, Myers JR, Ashton JM, Stewart RA, Featherston AL, Gates K, Helms ED, Smith HC, Dewhurst S, and Miller BL. HIV-1 frameshift RNA-targeted triazoles inhibit propagation of replication-competent and multi-drug-resistant HIV in human cells. ACS Chem. Biol, 12(6):1674–1682, 2017.

[70]. Toews S, Donà F, Keller M, Krauß J, Bracher F, López-García Ú, Pabel J, Merk D, Blommers MJJ, Ferner J, Wacker A, Richter C, and Schwalbe H. Targeting the sars-cov-2 rna translation initiation element sl1 by molecules of low molecular weight. J. Am. Chem. Soc, 147(32):28783–28798, 2025.

[71]. Masotti A. Beyond variant evolution: Structurally and functionally conserved regions in the 5'utr of sars-cov-2 as resilient antiviral targets. Biomedicines, 14(3):622, 2026.

[72]. Gi Byun W, Lee M, Ko M, Hyae Lee J, Yi S, Lee J, Kim S, and Bum Park S. Broad-Spectrum Antiviral Agents against SARS-CoV-2 Variants Inhibit the Conserved Viral Protein Nsp1–RNA Interaction. Angew. Chem. Int. Ed, 63(47):e202405472, 2024.

[73]. Hermann T. Small molecules targeting viral RNA. WIREs RNA, 7:726–743, 2016.

Author Manuscript Author Manuscript Author Manuscript Author Manuscript

[74]. Nguyen TM, Zhang Y, and Pandolfi PP. Virus against virus: a potential treatment for 2019-nCov(SARS-CoV-2) and other RNA viruses. Cell Res., 30:189–190, 2020.

[75]. Miao Z, Adamiak R, Antczak M, Boniecki M, Bujnicki J, et al. RNA-Puzzles Round IV: 3D structure predictions of four ribozymes and two aptamers. RNA, 26(8):982–995, 2020.

[76]. Sun L, Zhang D, and Chen S. Theory and modeling of RNA structure and interactions with metal ions and small molecules. Annu. Rev. Biophys, 46(1):227–246, 2017.

[77]. Roeder K, Stirnemann G, Meuret L, Barquero-Morera D, Forget S, Wales DJ, and Pasquali S. Exploring rna conformational ensembles in silico: progress and challenges. bioRxiv, 2026.

[78]. Languin-Cattoën O and Bussi G. Rna dynamics and interactions revealed through atomistic simulations. Annu Rev Phys Chem, 77(1):489–512, 2026.

[79]. Pekarek L, Zimmer MM, Gribling-Burrer A-S, Buck S, Smyth R, and Caliskan N. Cis-mediated interactions of the SARS-CoV-2 frameshift RNA alter its conformations and affect function. Nucleic Acids Res., 51(2):728–743, 2023.

[80]. Allen S, Schlick T, and Laederach A. RNA structural ensemble determinants of −1 programmed ribosomal frameshifting efficiency across coronavirus evolution. J. Mol. Biol, 437(24):169512, 2025.

[81]. Choi J, O'Loughlin S, Atkins JF, and Puglisi JD. The energy landscape of 1 ribosomal frameshifting. Sci. Adv, 6(1):eaax6969, 2020.

[82]. Dey A, Yan S, Schlick T, and Laederach A. Abolished frameshifting for predicted structure-stabilizing SARS-CoV-2 mutants: Implications to alternative conformations and their statistical structural analyses. RNA, 30(11):1437–1450, 2024.

[83]. Todisco M, Ding D, and Szostak JW. Transient states during the annealing of mismatched and bulged oligonucleotides. Nucleic Acids Res., 52(5):2174–2187, 2024.

[84]. Halma MTJ, Ritchie DB, Cappellano TR, Neupane K, and Woodside MT. Complex dynamics under tension in a high-efficiency frameshift stimulatory structure. Proc. Nat. Acad. Sci. USA, 116(39):19500–19505, 2019.

[85]. Yan S and Schlick T. Heterogeneous and multiple conformational transition pathways between pseudoknots of the SARS-CoV-2 frameshift element. Proc. Natl. Acad. Sci. USA, 122(4):e2417479122, 2025.

[86]. Hsu C-F, Chang K-C, Chen Y-L, Hsieh P-S, Lee A-I, Tu J-Y, Chen Y-T, and Wen J-D. Formation of frameshift-stimulating RNA pseudoknots is facilitated by remodeling of their folding intermediates. Nucleic Acids Res., 49(12):6941–6957, 2021.

[87]. Neupane K, Zhao M, Lyons A, Munshi S, Ileperuma SM, Ritchie DB, Hoffer NQ, Narayan A, and Woodside MT. Structural dynamics of single SARS-CoV-2 pseudoknot molecules reveal topologically distinct conformers. Nature Comm., 12:4749, 2021.

[88]. Caliskan N, Katunin VI, Belardinelli R, Peske F, and Rodnina MV. Programmed −1 frameshifting by kinetic partitioning during impeded translocation. Cell, 157(7):1619–1631, 2014.

[89]. Chen J, Petrov A, Johansson M, Tsai A, O'Leary SE, and Puglisi JD. Dynamic pathways of −1 translational frameshifting. Nature, 512(7514):328–332, 2014.

[90]. Madden EA, Plante KS, Morrison CR, Kutchko KM, Sanders W, Long KM, Taft-Benz S, Cruz Cisneros MC, White AM, Sarkar S, Reynolds G, Vincent HA,Laederach A, Moorman NJ, and Heise MT. Using shape-map to model rna secondary structure and identify 3'utr variation in chikungunya virus. J. Virol, 95(24):e00701–20, 2020.

[91]. Mikkelsen AA, Gao F, Carino E, Bera S, and Simon AE. −1 programmed ribosomal frameshifting in class 2 umbravirus-like rnas uses multiple long-distance interactions to shift between active and inactive structures and destabilize the frameshift stimulating element. Nucleic Acids Res., 51(19):10700–10718, 2023.

[92]. Lee S, Yan S, Dey A, Laederach A, and Schlick T. A cascade of conformational switches in sars-cov-2 frameshifting: Coregulation by upstream and downstream elements. Biochem., 64(4):953–966, 2025.

[93]. Bhatt PR, Scaiola A, Loughran G, Leibundgut M, Kratzel A, Meurs R, Dreos R, O'Connor KM, McMillan A, Bode JW, Thiel V, Gatfield D, Atkins JF, and Ban N. Structural basis of ribosomal frameshifting during translation of the SARS-CoV-2 RNA genome. Science, 372(6548):1306–1313, 2021.

Author Manuscript Author Manuscript Author Manuscript Author Manuscript

[94]. Olson SW, Turner A-MW, Arney JW, Saleem I, Weidmann CA, Margolis DM, Weeks KM, and Mustoe AM. Discovery of a large-scale, cell-state-responsive allosteric switch in the 7SK RNA using DANCE-MaP. Mol. Cell, 82(9):1708–1723.e10, 2022.

[95]. Mustoe AM, Weidmann CA, and Weeks KM. Single-molecule correlated chemical probing: A revolution in RNA structure analysis. Acc. Chem. Res, 56(7):763–775, 2023.

[96]. Arney JW, Laederach A, and Weeks KM. Visualizing rna structure ensembles by single-molecule correlated chemical probing. Curr. Opin. Struct. Biol, 88:102877, 2024.

[97]. Zubradt M, Gupta P, Persad S, M Lambowitz A, Weissman JS, and Rouskin S. Dms-mapseq for genome-wide or targeted rna structure probing in vivo. Nat Methods, 14(1):75–82, 2017.

[98]. Pekarek L, Zimmer MM, Gribling-Burrer A-S, Buck S, Smyth R, and Caliskan N. Cis-mediated interactions of the sars-cov-2 frameshift rna alter its conformations and affect function. Nucleic Acids Res., 51(2):728–743, 2023.

[99]. Lempereur L, Nicoloso M, Riehl N, Ehresmann C, Ehresmann B, and Bachellerie JP. Conformation of yeast 18s rrna. direct chemical probing of the 5' domain in ribosomal subunits and in deproteinized rna by reverse transcriptase mapping of dimethyl sulfate-accessible. Nucleic Acids Res., 13(23):8339–8357, 1985.

[100]. Tijerina P, Mohr S, and Russell R. Dms footprinting of structured rnas and rna-protein complexes. Nat Protoc, 2(10):2608–2623, 2007.

[101]. Mustoe AM, Weidmann CA, and Weeks KM. Single-molecule correlated chemical probing: A revolution in rna structure analysis. Acc Chem Res, 56(7):763–775, 2023.

[102]. Arney JW, Laederach A, and Weeks KM. Visualizing rna structure ensembles by single-molecule correlated chemical probing. Curr Opin Struct Biol, 88:102877, 2024.

[103]. Morandi E, Manfredonia I, Simon LM, Anselmi F, van Hemert MJ, Oliviero S, and Incarnato D. Genome-scale deconvolution of rna structure ensembles. Nat Methods, 18(3):249–252, 2021.

[104]. Tomezsko PJ, D A Corbin V, Gupta P, Swaminathan H, Glasgow M, Persad S, Edwards MD, Mcintosh L, T Papenfuss A, Emery A, Swanstrom R, Zang T, C T Lan T, Bieniasz P, R Kuritzkes D, Tsibris A, and Rouskin S. Determination of rna structural diversity and its role in hiv-1 rna splicing. Nature, 582(7812):438–442, 2020.

[105]. Schlick T and Yan S. Modeling and simulating RNA: Combining structural, dynamic, and evolutionary perspectives for coronavirus applications. In Laaksonen A and Mocci F, editors, Comprehensive Computational Chemistry. Elsevier, 2023.

[106]. Schlick T. Molecular Modeling: An Interdisciplinary Guide. Springer, New York, second edition, 2010.

[107]. Schlick T. Adventures with RNA Graphs. Methods, 143:16–33, 2018.

[108]. Bayrak C, Kim N, and Schlick T. Using sequence signatures and kink-turn motifs in knowledge-based statistical potentials for RNA structure prediction. Nucleic Acids Res., 45:5414–5422, 2017.

[109]. Meng G, Tariq M, Jain S, Elmetwaly S, and Schlick T. RAG-Web: RNA structure prediction/design using RNA-As-Graphs. Bioinform., 36:647–648, 2020.

[110]. Baba N, Elmetwaly S, Kim N, and Schlick T. Predicting large RNA-like topologies by a knowledge-based clustering approach. J. Mol. Biol, 428:811–823, 2016.

[111]. Jain S, Zhu Q, Paz ASP, and Schlick T. Identification of novel RNA candidates by clustering the extended RNA-As-Graphs library. Biochim. Biophys. Acta, 1864:129534, 2020.

[112]. Zbib J and Schlick T. Viral RNAs as dual graphs: Extending the motif universe of RNAs. Submitted, 2026.

[113]. Wang R and Schlick T. How large is the universe of RNA-like motifs? a clustering analysis of RNA graph motifs using topological descriptors. PLoS Comp. Biol, 21(7):e1013230, 2025.

[114]. Meng G, Tariq M, Jain S, Elmetwaly S, and Schlick T. RAG-Web: RNA structure prediction/design using RNA-As-Graphs. Bioinform., 36(2):647–648, 2019.

[115]. Jain S and Schlick T. F-RAG: Generating atomic coordinates from RNA graphs by fragment assembly. J. Mol. Biol, 429:3587–3605, 2017.

[116]. Zahran M, Bayrak C, Elmetwaly S, and Schlick T. RAG-3D: A search tool for RNA 3D substructures. Nucl. Acids Res, 43:9474–9488, 2015.

Author Manuscript Author Manuscript Author Manuscript Author Manuscript

[117]. Jain S, Bayrak CS, Petingi L, and Schlick T. Dual graph partitioning highlights a small group of pseudoknot-containing submotifs in RNAs. Genes, 9(8):371, 2018.

[118]. Kim N, Zheng Z, Elmetwaly S, and Schlick T. RNA graph partitioning for the discovery of RNA modularity: A novel application of graph partition algorithm to biology. PLoS One, 9(9):e106074, 2014.

[119]. Petingi L and Schlick T. Graph-theoretic partitioning of RNAs and classification of pseudoknots. In Holmes Ian, Martín-Vide Carlos, and Vega-Rodríguez Miguel A., editors, Algorithms for Computational Biology, pages 68–79, Cham, 2019. Springer International Publishing.

[120]. Kim N, Laing C., Elmetwaly S, Jung S, Curuksu J, and Schlick T. Graph-based sampling approach for approximating global helical topologies of RNA. Proc. Natl. Acad. Sci. USA, 111(11):4079–4084, 2014.

[121]. Omar S, Zhao M, Sekar R, Moghadam S, Tuszynski J, and Woodside M. Modeling the structure of the frameshift-stimulatory pseudoknot in SARS-CoV-2 reveals multiple possible conformers. PLOS Comput. Biol, 17:e1008603, 2021.

[122]. Deigan K, Li T, Mathews D, Weeks K, and Tinoco I. Accurate SHAPE-directed RNA structure determination. Proc. Natl. Acad. Sci. USA, 106(1):97–102, 2009.

[123]. Smola M and Weeks K. In-cell RNA structure probing with SHAPE-MaP. Nat. Protoc, 13(6):1181–1195, 2018.

[124]. Wacker A, Weigand J, Akabayov S, Altincekic N, Bains J, et al. Secondary structure determination of conserved SARS-CoV-2 RNA elements by NMR spectroscopy. Nucleic Acids Res., 48(22):12415–12435, 2020.

[125]. Hernández-Marín M, Cantero-Camacho Á, López-Núñez S Mena I, García-Sastre A,, and Gallego J. Sarbecovirus programmed ribosome frameshift RNA element folding studied by NMR spectroscopy and comparative analyses. Nucleic Acids Res., 52(19):11960–11972, 2024.

[126]. Peterson JM, Becker ST, O'Leary CA, Juneja P, Yang Y, and Moss WN. Structure of the SARS-CoV-2 frameshift stimulatory element with an upstream multibranch loop. Biochem., 63(10):1287–1296, 2024.

[127]. He W, San Emeterio J, Woodside MT, Kirmizialtin S, and Pollack L. Atomistic structure of the SARS-CoV-2 pseudoknot in solution from saxs-driven molecular dynamics. Nucleic Acids Res., 51(20):11332–11344, 2023.

[128]. Rangan R, Zheludev I, Hagey R, Pham E, Wayment-Steele H, Glenn J, and Das R. RNA genome conservation and secondary structure in SARS-CoV-2 and SARS-related viruses: a first look. RNA, 26(8):937–959, 2020.

[129]. Ziv O, Price J, Shalamova L, Kamenova T, Goodfellow I, Weber F, and Miska E. The short- and long-range RNA-RNA interactome of SARS-CoV-2. Mol. Cell, 80(6):1067–1077.e5, 2020.

[130]. Plant EP, Pérez-Alvarado GC, Jacobs JL, Mukhopadhyay J, Hennig M, and Dinman JD. A three-stemmed mRNA pseudoknot in the sars coronavirus frameshift signal. PLoS Biol., 3(6):e172, 2005.

[131]. Ishimaru D, Plant EP, Sims AC, Yount BL Jr., Roth BM, Eldho NV, Pérez-Alvarado GC, Baric RS, and Taylor DR. RNA dimerization plays a role in ribosomal frameshifting of the sars coronavirus. Nucleic Acids Res., 41(4):2594–2608, 2013.

[132]. Jain S, Tao Y, and Schlick T. Inverse folding with RNA-As-Graphs produces a large pool of candidate sequences with target topologies. J. Struct. Biol, 209:107438, 2020.

[133]. Lee S and Schlick T. Kinetic traps in rna folding: Targeted design of frameshifting eleemnt mutants by thermodynamic and kinetic analysis of the chikungunya virus. J. Phys. Chem, 130(6):1810–1831, 2026.

[134]. Newton K Yan S and Schlick T. Conformational analysis and structure-altering mutations of the HIV-1 frameshifting element. Int. J. Mol. Sci, 26(13):6297, 2025.

[135]. Chen S. Graph, pseudoknot, and SARS-CoV-2 genomic RNA: A biophysical synthesis. Biophys. J, 120:980–982, 2021.

Author Manuscript Author Manuscript Author Manuscript Author Manuscript

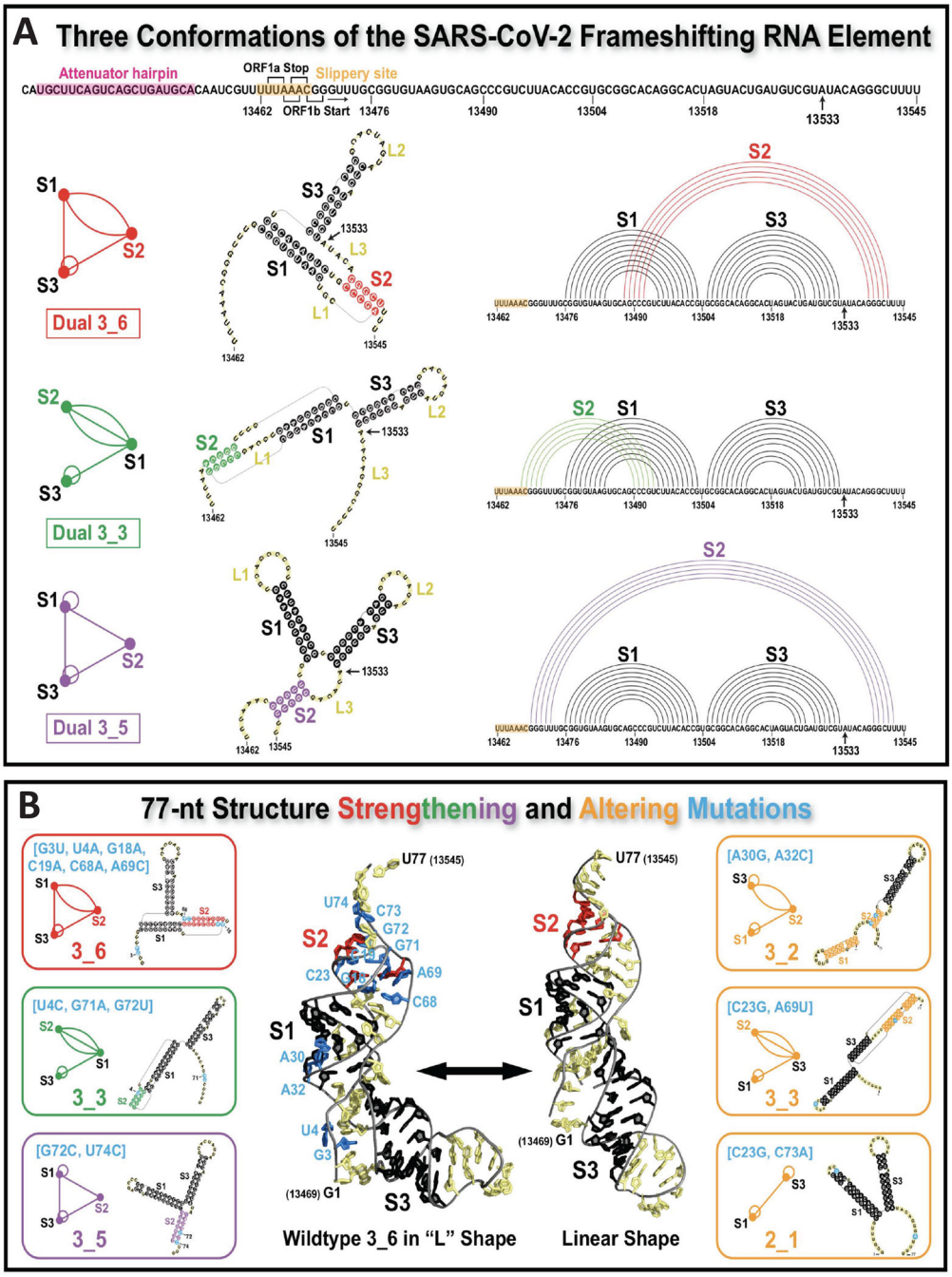


Figure 1: FSE sequence, three relevant 2D structures for the SARS-CoV-2 84 nt FSE (residues 13462–13545) emerging from our works [30, 31] and mutants that transform the 3_6 motif and stabilize all conformers, using graph-based models, 2D structure prediction, SHAPE structural probing, thermodynamic ensemble modeling, and molecular dynamics simulations [32].

A. The −1 frameshifting moves the transcript UUU-UU*A(Leu)-AAC(Asn)-GGG at the second codon (asterisk) to start as AAA-CGG(Arg), so that translation resumes at CGG. Top: FSE sequence, with the attenuator hairpin region, the 7 nt slippery site, and A13533 labeled (C in SARS). The ORF1a end and ORF1b start codons for the overlapping regions are marked. For each 2D structure, 3_6 pseudoknot, 3_3 pseudoknot, and three-way junction

Author Manuscript Author Manuscript Author Manuscript Author Manuscript

3_5 (unknotted RNA), we show corresponding dual graphs, 2D structures, and arc plots, with color-coded stems and loops. B, Left: Mutants that stabilize each conformer; B, Right: Double mutants that transform the 3_6 form into other RNAs. B, Middle: Straight to L-shape transition captured in our simulation for wildtype 3_6 system, which is suppressed in our 3_6 stabilizing mutant. This figure was adapted from [33].

Author Manuscript Author Manuscript Author Manuscript Author Manuscript

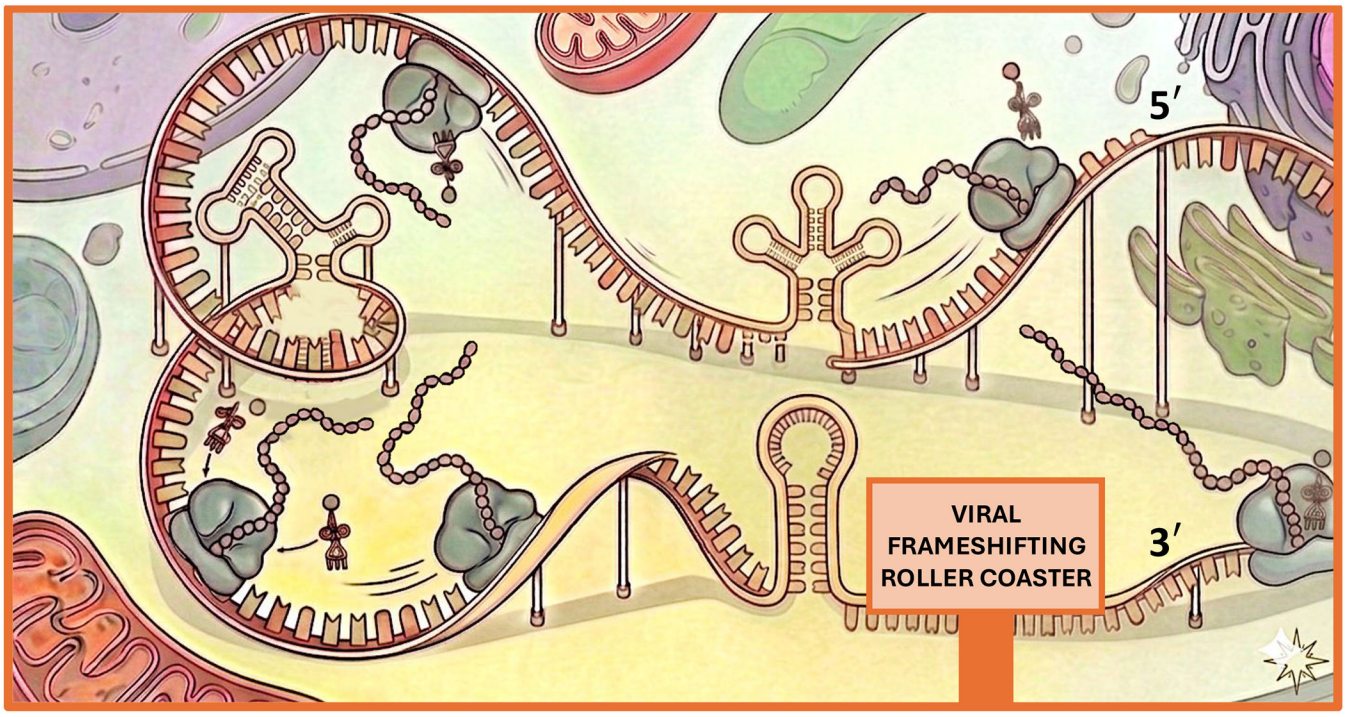


Figure 2: Viral RNA transcript as encountered by translating ribosomes depicted as a roller coaster.

This cartoon generated with the aid of Google Gemini AI depicts the RNA viral transcript with various folded regions as a “roller-coaster” with multiple translating ribosomes. Near the −1 PRF region, the exposed RNA will be folded, and the folds may change depending on the exposed RNA transcript available, that is, not occluded by ribosomes. In this way, multiple folds may be associated with the FSE and, depending on the sequence available, the RNA may fold and refold. Thus, following RNA folds as the sequence increases by adding upstream (5′) residues in computed conformational landscapes (see other figures) reveals structures available to the ribosome before it has passed the stimulatory region. The depicted folds are schematic and could occur in other template regions as well.

Author Manuscript Author Manuscript Author Manuscript Author Manuscript

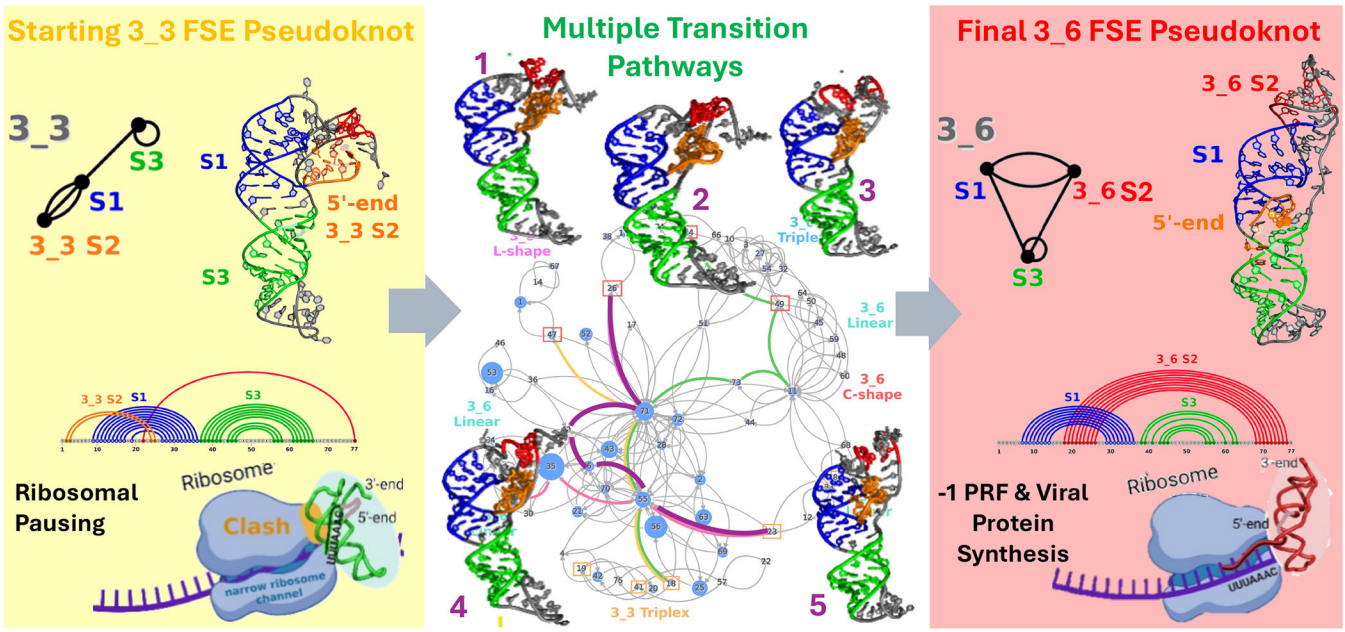


Figure 3: SARS-CoV-2 RNA frameshifting dynamics: Heterogeneous transition pathways delineated by atomic-level transition path sampling simulations of the FSE transition between two pseudoknots governing frameshifting [85].

This figure depicts the simulated transition from the starting 3_3 to the final 3_6 pseudoknot. It illustrates the multi-hub pathway network obtained by Markov State Modeling, with breaking of the initial pseudoknot stem emerging as the highest barrier in most transition paths. This pseudoknot transition is triggered by the spacer region tension, and accomplishes a good fit within the narrow ribosomal channel,as determined by alignment with the Cryo-EM structure [93].

Author Manuscript Author Manuscript Author Manuscript Author Manuscript

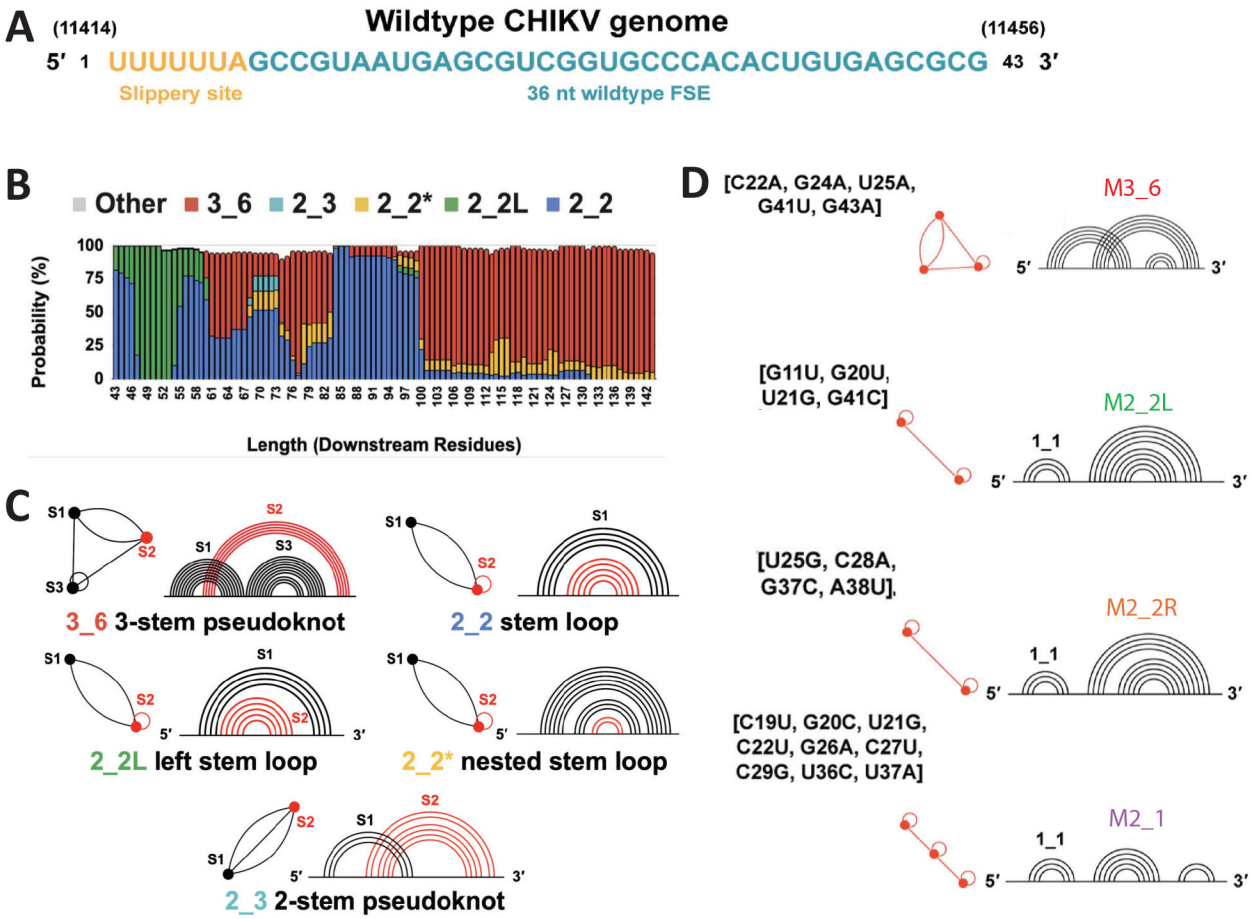


Figure 4: FSE sequence, conformational landscape with representative RNA folds, and associated mutant designs for the Chikungunya virus (CHIKV) [133].

A. FSE site sequence context for CHIKV. B. CHIK downstream landscape showing the fold population as a function of RNA length, with colors corresponding to the fold classes depicted for landscape classification as coarse-grained dual graphs. C. Key folds associated with the landscape in B. D. Designed mutant systems for selected target motifs shown as dual graphs. Resulting folds are also shown as arc plots. These mutants were revised to reflect our integrative pipeline which includes kinetics analysis to eliminate kinetic traps. The residue numbers correspond to residues labeled in A from 1 to 43. Figure adapted from images in [133].

Author Manuscript
Author Manuscript
Author Manuscript
Author Manuscript

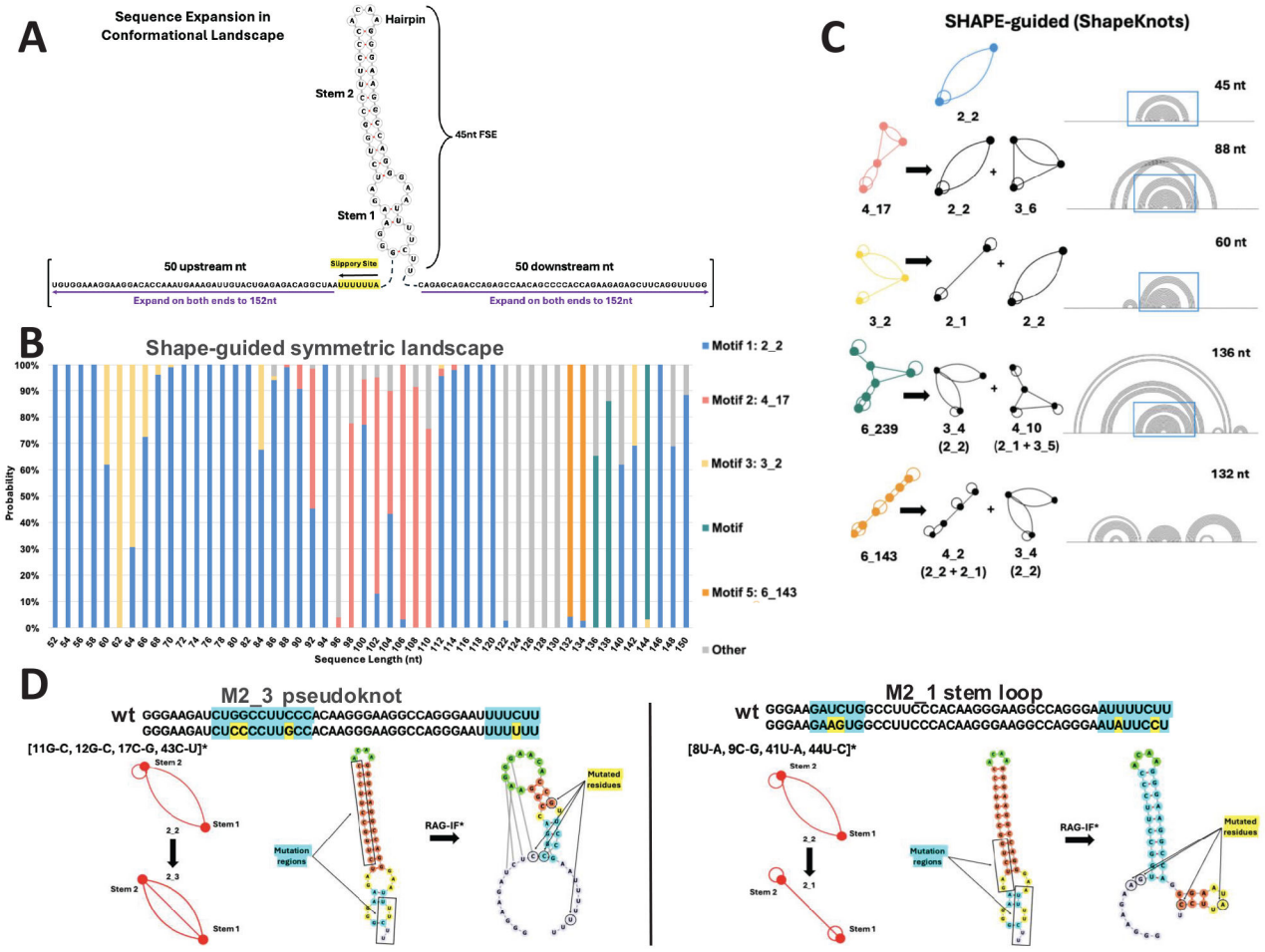


Figure 5: FSE sequence, conformational landscape with representative RNA folds, and associated mutant designs for the HIV-1 virus [134].

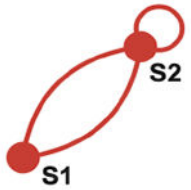
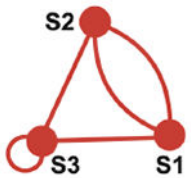
A. FSE site sequence context for HIV-1. B. HIV-1 symmetric expansion landscape (added upstream and downstream residues) guided by SHAPE chemical-reactivity data as restraints showing the fold population as a function of RNA length, with colors corresponding to fold classes depicted as coarse-grained dual graphs. C. Key folds associated with the landscape in B and their partitioning into irreducible subgraphs, with arc plots representing folds for specific lengths of RNAs. The core sequence is 45nt (see A). D. Designed mutant systems for selected target motifs. Figure adapted from images in [134].

Author Manuscript Author Manuscript Author Manuscript Author Manuscript

Biophys J. Author manuscript; available in PMC 2026 May 22.

Table 1:

Experimentally determined 3D structures of representative viral frameshifting elements (FSEs) and related PRF-stimulatory pseudoknots. PDB IDs and primary structure papers are cited in the last column.

Motif	Graph	Virus (FSE)	PRF	Reported eff.	Method	PDB / primary structure reference
Dual 2_2 Stem-loop		HIV-1	−1	~10%	NMR	1Z2J [34] (eff.: [35])
		SIV	−1	~8%	NMR	2JTP [36]
		PEMV-1	−1	~9%	NMR	1KPZ [37]
Dual 2_3 Pseudoknot		PLRV	−1	~ 9%	X-ray	2A43 [38]
		ScYLV	−1	~15%	NMR	1YG4 [39]
		BWYV	−1	~11%	X-ray	1L2X [40]
		MMTV	−1	~20%	NMR	1RNK [41]
		SRV-1	−1	~23%	NMR	1E95 [42]
Dual 3_6 Pseudoknot		SARS-CoV-2	−1	~20%	X-ray / Cryo-EM	7MLX [43]; 6XRZ [22]; 7O7Z [44]; 7LYJ/7MKY [45]

Author Manuscript
Author Manuscript
Author Manuscript
Author Manuscript

Motif	Graph	Virus (FSE)	PRF	Reported eff.	Method	PDB / primary structure reference
Dual 5_55/6_105 * Double-pseudoknot		RSV	−1	~ 6%	X-ray/ Cryo-EM	9DIB; 9DID; 9DIG; 9DII [46]

* This FSE has two different conformations where one has an extra small helix. Crystal packing may impact these findings. See Figure 1 of Ref. [46].